

# An efficient enzymatic approach for the detection of glucose and uric acid from blood serum

Sourav Bhowmik, Sagar Biswas and Apurba K. Das\*

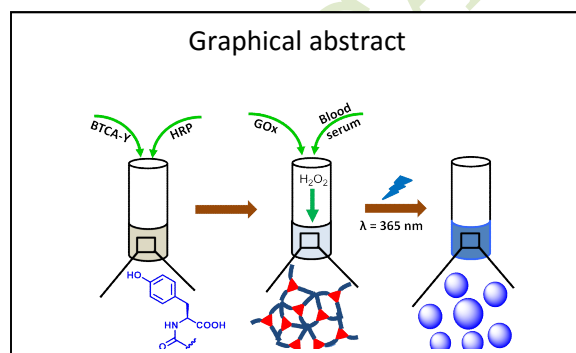
Department of Chemistry, Indian Institute of Technology Indore, Indore 453552, India  
Email: apurba.das@iiti.ac.in

Received: March 30, 2023 | Accepted: June 05, 2023 | Published online: \*\*\*\*

## Abstract

Hydrogen peroxide ( $H_2O_2$ ) is one of the significant reactive oxygen species (ROS) in living organisms, which is produced through mitochondrial respiration. The aberrant generation of  $H_2O_2$  leads to complex diseases. The current study is focused on the preparation of highly effective fluorescent biopolymeric organic nanoparticles for the detection of  $H_2O_2$ . The synthesized compounds are highly selective towards  $H_2O_2$  in presence of an enzyme horseradish peroxidase (HRP). In-situ generation of fluorogenic polymeric NPs by enzymatic cascade reactions recognize  $H_2O_2$  in blood serum. This novel approach is suitable for the detection of elevated glucose and uric acid in blood serum in case of diabetic and gout condition through  $H_2O_2$  detection. This method could hold the place of future diagnostic tool for various complex diseases including diabetes and gout.

**Keywords:** Hydrogen peroxide, enzyme, cascade reaction, polymeric fluorescent sensor, glucose and uric acid sensing



## 1. Introduction

Aerobic respiration of increased biological substances (bioanalytes) including cholesterol, lactate, choline, glutamate, alcohol, glucose and uric acid produces a significant amount of reactive oxygen species (ROS) that are potent oxidizing agents in the living organisms.<sup>1-3</sup> Hydrogen peroxide ( $H_2O_2$ ), known as one of the major ROS in living body, is considered to be generated largely through mitochondrial respiration.<sup>4-6</sup>  $H_2O_2$  is a common cellular signaling marker in a variety of biological processes while aberrant generation of  $H_2O_2$  leads to oxidative stress, inflammation in ageing, injury and neurodegenerative diseases including Parkinson's and Alzheimer's diseases.<sup>7-10</sup> The necessity of precise detection of biological  $H_2O_2$  inspires researchers to develop various sensing techniques.<sup>11-16</sup> The fluorometric method is one of the most applied and more accurate sensitive methods.<sup>5,17-21</sup> Including fluorogenic methods, several small molecule-based reversible sensors were also reported earlier for the detection of  $H_2O_2$  [22-25]. To date, researchers aimed at various  $H_2O_2$  labile functionalities i.e., benzil, benzene sulfonyl ester and boronate ester as the chemical tool to design fluorogenic probes for studying  $H_2O_2$  concentration in biological system.<sup>3,26-28</sup> Early developed reaction based on fluorogenic  $H_2O_2$  probes offers great merits which have few limitations including insufficient solubility in water at physiological conditions, long incubation periods, detection of limited bioanalytes and low selectivity over other ROS (e.g., TBHP,  $\dot{O}H$  and  $\dot{O}tBu$ ). Naked eye detection of multiple bioanalytes along with fluorogenic response at biological condition over

narrow time range is also an advantage which needs more exploration.

Including various fluorogenic probes, fluorescent polymeric nanospheres also emerge considerable interest for the development of chemosensors as well as biosensors for the cellular signaling molecule.<sup>29,30</sup> Most of the polymers have been used directly for  $H_2O_2$  detection whereas few reports on in-situ polymerization to recognize biological  $H_2O_2$  through fluorogenic response also inscribed in the literature.<sup>31</sup> In-situ formation of fluorescent polymers is more promising over externally synthesized polymer as the former is formed in one-pot.<sup>32,33</sup> Meanwhile, fluorescent polymeric probes composed of bioactive molecules have a significant advantage over abiotic polymeric probes due to their biocompatibility and biodegradability.<sup>34</sup> Unlike conventional in-situ polymerization method, enzymatic cross-linking is one of the leading approaches for the polymerization of biomolecules for several applications in biotechnology.<sup>35</sup>

Numerous classes of enzymes e.g., peroxidase, proteinase and hydrolase actively participate to form regioselective cross-linked polymeric networks.<sup>36-38</sup> Horseradish peroxidase (HRP) is a promising redox active peroxidase enzyme that requires  $H_2O_2$  to oxidize phenolic -OH containing molecules and cross-linked through radical formation.<sup>39-41</sup> Several HRP catalyzed effective  $H_2O_2$  detection probes were mentioned earlier.<sup>39</sup> However, in-situ polymeric fluorescent probe using biomolecules, and a single platform for multiple bioanalytes (glucose and uric acid) detection have not been focused. Functionalized 1,3,5-benzenetricarboxamide (BTCA) can serve multi branches for an extended polymeric network on

cross-linking.<sup>40</sup> The use of aromatic carboxylic ligands such as BTCA is advantageous and used by most of the chemists. It has a rigid cyclic skeleton which helps to form the multidimensional structure. In addition to, the conjugated system of aromatic cycle also facilitates the transfer of electron. BTCA is not considered as a fluorescent probe because of its inadequate fluorescence response. However, BTCA could be easily functionalized to prepare a significant fluorescent probe, which could be used for the detection of bio-analytes. Herein, our approach stands on the development of tyrosine functionalized BTCA-based monomer for the formation of fluorescent polymer on the response of H<sub>2</sub>O<sub>2</sub> producing from different biological sources. Enzyme-cascade is a series of enzymatic reactions that runs parallel so, enzyme cascade allows us to detect multiple bio-analytes in blood serum in the same platform.

## 2. Experimental

**Synthesis of BTCA-Y-OMe (compound 1):** 300 mg (1.42 mmol) of 1,3,5-benzenetricarboxylic acid was dissolved in 1.5 mL of N, N-dimethylformamide (DMF) and cooled in an ice bath. H<sub>2</sub>N-Tyr-OMe was freshly obtained from 1.17 g (5.08 mmol) of its corresponding ester hydrochloride. The ester hydrochloride was dissolved in the deionized water and the neutralization was carried out by the dropwise addition of sodium carbonate (Na<sub>2</sub>CO<sub>3</sub>). It was extracted with ethyl acetate and evaporated under vacuum, finally it was added into the reaction mixture, then 972 mg (4.71 mmol) of dicyclohexylcarbodiimide (DCC) and the activator HOBt, 578 mg (4.28 mmol) were added into the reaction mixture. The reaction mixture was kept at room temperature and stirred for overnight. The progress of the reaction was monitored by the thin layer chromatography (TLC). After the completion of the reaction, the reaction mixture was diluted with 50 mL of ethyl acetate. The filtration was done to remove dicyclohexylurea (DCU) from the reaction mixture. The organic layer was washed with 1 M HCl (3×50 mL), 1 M sodium carbonate (3×50 mL), and brine (2×50 mL), dried over anhydrous sodium sulphate, and evaporated under vacuum to yield white solid. Further the purification of the compound was carried out by flash chromatography using ethyl acetate and hexane as eluent.

Yield: 1.47 g (1.98 mmol, 91%); <sup>1</sup>H NMR (400 MHz, DMSO-d<sub>6</sub>): δ 9.21 (s, 3H, -OH of Tyr), 9.12-9.11 (d, 2H, *J* = 7.08 Hz, -NH), 8.38 (s, 3H, BTC ring -Hs), 7.09-7.07 (d, 6H, *J* = 8.24 Hz, Tyr ring -Hs), 6.67-6.65 (d, 6H, *J* = 8.24 Hz, Tyr ring -Hs), 4.62-4.57 (m, 3H, C<sup>α</sup>H of Tyr), 3.63 (s, 9H, -OMe of Tyr), 3.07-2.97 (m, 6H, C<sup>β</sup>H of Tyr) ppm. MS (ESI) *m/z* for C<sub>39</sub>H<sub>39</sub>N<sub>3</sub>O<sub>12</sub> (M+Na)<sup>+</sup> calcd.: 764.56, found: 764.56.

**Synthesis of BTCA-Y-OH (BTCA-Y):** A solution of 1 g (1.31 mmol) BTCA-Y-OMe was dissolved in 5 mL of distilled methanol. Then, 5 mL of 1 (N) NaOH solution was added in the reaction mixture. Then, the reaction mixture was left for stirring upto 4h. The reaction progress of the hydrolysis was monitored by TLC. The excess methanol was evaporated under vacuum, when the reaction was completed. Then the reaction mixture was diluted with 100 mL of water. The

mixture was then transferred into a separating funnel and washed vigorously with diethyl ether. The aqueous layer was taken in a conical flask and cooled under ice bath. Then, the cooled water part was acidified with the gradual addition of 1 (N) KHSO<sub>4</sub>. The pH of aqueous layer was adjusted to 2 and the product was extracted with ethyl acetate (3×30 mL). The ethyl acetate layer was dried over anhydrous sodium sulphate and evaporated under reduced pressure to obtain solid compound **BTCA-Y-OH**.

Yield: 0.89 g (1.28 mmol, 98%) <sup>1</sup>H NMR (400 MHz, DMSO-d<sub>6</sub>): δ 12.72 (s, 3H, -COOH) 9.18 (s, 3H, -OH of Tyr), 8.95-8.93 (d, 2H, *J* = 7.08 Hz, -NH), 8.34 (s, 3H, BTC ring -Hs), 7.11-7.09 (d, 6H, *J* = 8.24 Hz, Tyr ring -Hs), 6.67-6.65 (d, 6H, *J* = 8.24 Hz, Tyr ring -Hs), 4.59-4.54 (m, 3H, C<sup>α</sup>H of Tyr), 3.10-2.94 (m, 6H, C<sup>β</sup>H of Tyr) ppm. <sup>13</sup>C NMR (100 MHz, DMSO-d<sub>6</sub>): δ 173.57 (for -COOH), 166.12 (-CONH<sub>2</sub>) 156.31 (aromatic ring C), 134.94 (aromatic ring C), 130.42 (aromatic ring C), 129.56 (aromatic ring C), 128.53 (aromatic ring C), 115.53 (aromatic ring C), 55.29 (C<sup>α</sup> of Tyr) and 36.02 (C<sup>β</sup> of Tyr) ppm. MS (ESI) *m/z* for C<sub>38</sub>H<sub>37</sub>N<sub>3</sub>O<sub>11</sub> (M+Na)<sup>+</sup> calcd.: 722.20 found: 722.20.

**Synthesis of Boc-GY-OMe (compound 3):** 470 mg (2.68 mmol) Boc-G-OH (**compound 2**) was taken in a 100 mL round bottom flask and it was then allowed to cool on ice bath. Then 608 mg (2.95 mmol) DCC was added to the stirring solution of Boc-G-OH. The H<sub>2</sub>N-Y-OMe was extracted from the 1.025 g (4.02 mmol) of hydrochloride salt of tyrosine methyl ester and then added to the mixture followed by the addition of 362 mg (2.68 mmol) HOBt to the mixture. The procedure used to synthesize BTCA-Y-OMe was used to synthesize and purify Boc-GY-OMe.

Yield: 0.88 g (2.5 mmol, 93%), <sup>1</sup>H NMR (400 MHz, DMSO-d<sub>6</sub>): δ 9.27 (s, 1H, -OH of Tyr), 8.15-8.14 (d, 1H, *J* = 8 Hz, -NH), 7.03-7.01 (d, 2H, *J* = 8 Hz, ring -Hs of Tyr), 6.97-6.95 (m, 1H, -NH), 6.71-6.69 (d, 2H, *J* = 8 Hz, ring -Hs of Tyr), 4.48-4.43 (m, 1H, C<sup>α</sup>Hs of Tyr), 3.64 (s, 3H, -OMe), 3.58-3.56 (m, 2H, Gly -CH<sub>2</sub>), 2.95-2.82 (m, 2H, C<sup>β</sup>Hs of Tyr), 1.43 (s, 9H, -Boc group) ppm.

**Synthesis of H<sub>2</sub>N-GY-OMe (compound 4):** 0.8 g (2.27 mmol) of the Boc-GY-OMe was dissolved in trifluoroacetic acid (TFA) and kept for 3h under N<sub>2</sub> atmosphere. After completion of the reaction excess TFA was evaporated to dryness and the gummy solid was washed with cold ether to get white solid product. Then the ether layer was removed and the obtained solid was dried under vacuum.

Yield 0.55 g (2.2 mmol, 97%) <sup>1</sup>H NMR (400 MHz, DMSO-d<sub>6</sub>): δ 8.83-8.82 (d, 1H, *J* = 4 Hz, -NH), 8.03 (s, 2H, -NH<sub>2</sub>), 7.01-6.99 (d, 2H, *J* = 8 Hz, ring -Hs of Tyr), 6.69-6.67 (d, 2H, *J* = 8 Hz, ring -Hs of Tyr), 4.50-4.46 (m, 1H, C<sup>α</sup>Hs of Tyr), 3.62 (s, 3H, -OMe), 3.58-3.55 (m, 2H, Gly -CH<sub>2</sub>), 2.96-2.78 (m, 2H, C<sup>β</sup>Hs of Tyr) ppm.

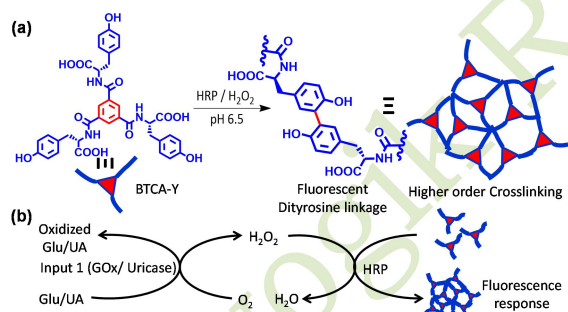
**Synthesis of BTCA-GY-OMe (compound 5):** 139 mg (0.66 mmol) of 1,3,5-benzenetricarboxylic acid was taken in a 50 mL R.B. It was dissolved in 1.5 mL of N, N-dimethylformamide (DMF). It was placed in an ice bath. 500

mg (1.98 mmol) of H<sub>2</sub>N-GY-OMe was directly added to the reaction mixture, followed by the addition of 310 mg (2 mmol) of 1-ethyl-3-(3-dimethylaminopropyl) carbodiimide (EDC) and 270 mg (2 mmol) of HOBt. The procedure used to synthesize BTCA-Y-OMe was used to synthesize and purify BTCA-GY-OMe.

Yield: 0.531 g (0.61 mmol, 92%), <sup>1</sup>H NMR (400 MHz, DMSO-d<sub>6</sub>): δ 9.08 (s, 3H, -OH of Tyr), 8.71 (s, 3H, -NH), 8.64 (s, 3H, Hs of BTC ring), 8.44-8.40 (m, 3H, -NH), 7.04-7.03 (d, 2H, J = 6.6 Hz, aromatic Hs of Tyr), 6.70-6.68 (d, 2H, J = 6.4 Hz, aromatic Hs of Tyr), 4.49-4.40 (m, 3H, C<sup>α</sup>Hs of Tyr), 3.97-3.93 (m, 6H, -CH<sub>2</sub> of Gly), 3.64 (s, 9H, -OCH<sub>3</sub>), 2.98-2.77 (m, 6H, C<sup>β</sup>Hs of Tyr) ppm.

**Synthesis of BTCA-GY-OH (BTCA-GY):** This compound was synthesized following the similar procedure as described earlier.

Yield: 286 mg (0.32 mmol, 96%); <sup>1</sup>H NMR (400 MHz, DMSO-d<sub>6</sub>): δ 9.33 (s, 3H, -OH of Tyr), 9.26 (s, 2H, -NH), 8.10 (s, 3H, BTC ring Hs), 7.87-7.82 (d, 3H, J = 16 Hz, -NH), 6.98-6.96 (d, 6H, J = 8 Hz, Tyr ring Hs), 6.70-6.68 (d, 6H, J = 8 Hz, Tyr ring Hs), 3.99 (s, 6H, -CH<sub>2</sub> of Gly), 3.61-3.54 (m, 3H, C<sup>α</sup>H of Tyr), 3.02-2.73 (m, 6H, C<sup>β</sup>Hs of Tyr) ppm. <sup>13</sup>C NMR (100 MHz, DMSO-d<sub>6</sub>): δ 173.39 (-COOH), 172.50 (-CONH<sub>2</sub>), 169.27 (-CONH<sub>2</sub>), 166.66 (aromatic ring C), 156.54 (aromatic ring C), 132.12 (aromatic ring C), 130.52 (aromatic ring C), 127.47 (aromatic ring C), 115.58 (aromatic ring C), 60.25 (C<sup>α</sup> of Tyr), 52.29 (C<sup>α</sup> of Gly) and 21.26 (C<sup>β</sup> of Tyr). MS (ESI) *m/z* for C<sub>39</sub>H<sub>39</sub>N<sub>3</sub>O<sub>12</sub> (M)<sup>+</sup> calcd.: 870.2, found: 870.2.



**Scheme 1.** (a) Schematic representation of HRP/H<sub>2</sub>O<sub>2</sub> mediated cross-coupling of BTCA-Y and formation of fluorescent tyrosine crosslinked polymeric network. (b) Overall cascade reaction pathways for glucose/uric acid with enzyme GOx and uricase respectively.

### 3. Results and discussion

To implement the hypothesis, two L-tyrosine functionalized discotic compounds were synthesized (BTCA-Y and BTCA-GY). The purity of compounds was checked by HPLC chromatograms (Figure S1). An amino acid residue Tyr (Y) and a dipeptide Gly-Tyr (GY) appended BTCA amphiphiles exhibit enhanced solubility in water. The tyrosine moiety cross-linked to each other in presence of H<sub>2</sub>O<sub>2</sub> to form crosslinked polymeric networks (Scheme 1) [42]. An enzyme HRP catalyzed reactions were performed using buffer

solution at different pHs (pH = 6, 6.5, 7, 8 and 9) to get better results (Figure S2).

Emission spectra were recorded ( $\lambda_{\text{ex}} = 290 \text{ nm}$ ) for the reaction mixtures at mentioned pHs and excellent sensing ability was obtained using 10 mM phosphate buffer solution of pH 6.5. Initially, BTCA-Y and BTCA-GY were dissolved in PB buffer solution with 3.5 U/mL HRP (Figure S3), and then gradually H<sub>2</sub>O<sub>2</sub> was added (from 0 to 100  $\mu\text{M}$ ) to reach the equilibrium (Figure 1). The fluorescence intensity at 410 nm plot against different concentrations of H<sub>2</sub>O<sub>2</sub> shows first rapid increase and then saturation to linearity on addition of 50  $\mu\text{M}$  of H<sub>2</sub>O<sub>2</sub> solution. The inset plot of Figure 1b with the initial concentration of H<sub>2</sub>O<sub>2</sub> (0 to 40  $\mu\text{M}$ ) fits to the linearity with R<sup>2</sup> value of 0.9935 (Figure 1b) which shows the characteristic feature of the enzymatic kinetics. The whole reaction was completed within a very short time (7 min) (Figure S3). The limit of detection (LOD) value of H<sub>2</sub>O<sub>2</sub> is calculated as 0.38  $\mu\text{M}$  using the method (LOD = 3  $\times$   $\sigma/m$ ,  $\sigma$  represents standard deviation of the response at the minimum tested concentration where *m* represents the slope of the concentration-dependent curve, here  $\sigma = 0.09671$ , *m* = 0.74963) reported by Li et al [1]. Few of best the reported H<sub>2</sub>O<sub>2</sub> detection probe reported earlier are tabulated and the LOD value is comparable to the best organic fluorescent probes reported by Liu et al (Table 1) [43]. On cross-linking of tyrosine moieties, both BTCA-Y and BTCA-GY form polymeric nanospheres. BTCA-Y exhibits emission maxima at 410 nm whereas BTCA-GY shows emission maxima at 416 nm upon polymerization ( $\lambda_{\text{ex}} = 290 \text{ nm}$ ). While comparing the increment of emission intensities; BTCA-Y dominates over BTCA-GY by ~2 times (Figure S4). Hence, to simplify this work, only BTCA-Y was taken under consideration for the detection of bio-analytes.

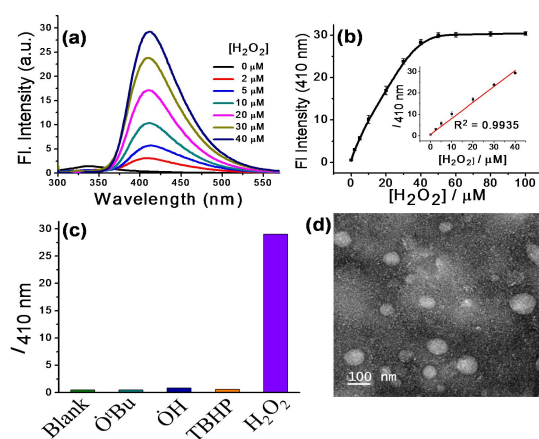


**Figure 1.** (a) Emission spectra of BTCA-Y solution at a concentration of 30  $\mu\text{M}$  in presence of 0-40  $\mu\text{M}$  of H<sub>2</sub>O<sub>2</sub>. (b) Fluorescence intensity vs concentration of H<sub>2</sub>O<sub>2</sub> (0-100  $\mu\text{M}$ ) plot and inset shows linear fitting curve. (c) Response of BTCA-Y at a concentration of 30  $\mu\text{M}$  to various ROS species and emission intensities at 410 nm. (d) TEM image of formed polymeric nanospheres after HRP at a concentration of 3.5 U/mL mediated crosslinking.  $\lambda_{\text{ex}} = 290 \text{ nm}$ ,  $\lambda_{\text{em}} = 410 \text{ nm}$ ; 7 min was fixed as reaction time in all the cases.

As HRP is highly selective towards the tyrosine moieties, [44] so, it was assumed that tyrosine moieties would be selectively cross-linked to each other by the assistance of H<sub>2</sub>O<sub>2</sub> respective to other ROSs (TBHP, *o*Tu, *o*H) (Figure 1c). The sensitivities of BTCA-Y towards other ROSs were checked by using TBHP, *o*Tu, *o*H at pH 6.5 in PB solution. However, BTCA-Y was responded by only H<sub>2</sub>O<sub>2</sub>. As BTCA-Y promises much significant emission intensity over BTCA-GY, so, further studies were performed only with BTCA-Y.

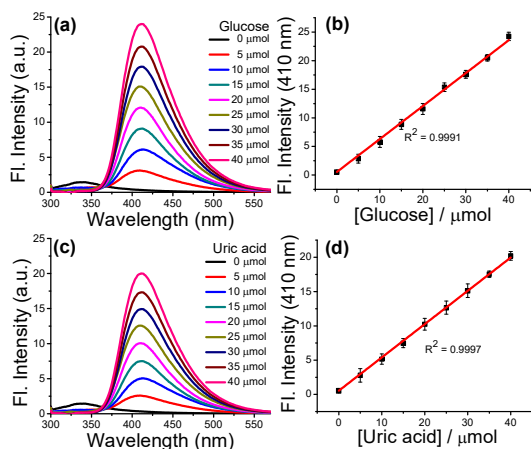


**Figure 2.** (a) Fluorescence spectra of GOx/HRP cascade system with various concentration of glucose (0 to 40  $\mu\text{mol mL}^{-1}$ ) and (b) fitting curve of the fluorescence response towards various concentration of glucose. (c) Represents the fluorescence spectra of UOx/HRP cascade system with uric acid of 0 to 40  $\mu\text{mol mL}^{-1}$  and (d) fitting curve of the fluorescence response towards various concentrations of uric acid.  $\lambda_{\text{ex}} = 290 \text{ nm}$ ,  $\lambda_{\text{em}} = 410 \text{ nm}$ ; 7 min was fixed as reaction time in all the cases.

**Table 1.** Earlier reports on the detection of H<sub>2</sub>O<sub>2</sub>

S. No	Developed system	LOD value in terms of H <sub>2</sub> O <sub>2</sub>	Purposes	References
1	Amino acid functionalized enzymatic polymeric probe	0.38 $\mu\text{M}$	Multianalyte detection in blood serum	Current work
2	TPE-BO fluorogenic probe	0.52 $\mu\text{M}$	Detection of H <sub>2</sub> O <sub>2</sub> in living cell	[45]
3	Polymeric nanoprobe based on ARS-FPBA	0.76 $\mu\text{M}$	Glucose detection	[29]
4	TPE-tyrosine based polymer probe	0.35 $\mu\text{M}$	Quantitative analysis of human CEA	[35]
5	Self-assembled polymeric nanoprobe	0.95 $\mu\text{M}$	Detection of mitochondrial H <sub>2</sub> O <sub>2</sub> in living cells	[46]

6	PEG-QDs based chemiluminescence	0.5 $\mu\text{M}$	In vivo imaging of H <sub>2</sub> O <sub>2</sub>	[47]
7	Cationic conjugated polymers	5 $\mu\text{M}$	Detection of glucose	[48]

TPE-BO = 1,2-diphenyl-1,2-bis[4-(4,4,5,5-tetramethyl-1,3,2-dioxaborolan-2-yl)phenyl]ethane; ARS-FPBA = alizarin red S-(4-carboxy-3-fluorophenylboronic acid); TPE-tyrosine = tetraphenylethylene-tyrosine; PEG-QDs = polyethyleneglycol-quantum dots.

The hydrodynamic radius of the formed polymeric nanospheres [49,50] upon enzymatic cross-linking was studied through DLS experiments. The DLS spectrum was acquired at pH 6.5 and the nanosphere formed with the diameter of  $106 \pm 2 \text{ nm}$  was observed from DLS (Figure S5). To visualize the surface morphology of the crosslinked polymers, transmission electron microscopy was performed. Polymeric nanospheres were observed having an average diameter of 100 nm for BTCA-Y cross-linked polymer (Figure 1d, Figure S5). The BTCA-Y has shown very high selectivity towards H<sub>2</sub>O<sub>2</sub> and it was chosen further for the detection of H<sub>2</sub>O<sub>2</sub> generated upon oxidation of biological substances.

### Development of Cascade System

To develop cascade system, 3.5 U/mL of glucose oxidase (GOx) and 4 U/mL of uricase were used in HRP mediated BTCA-Y solution at pH 6.5 (Figure S6). Cascade systems were developed in the mixture of 30  $\mu\text{M}$  BTCA-Y solutions with HRP. Later GOx or uricase was added individually to the solution. Glucose or uric acid concentrations were varied from 0 to 150  $\mu\text{mol mL}^{-1}$  (Figure S6). In case of HRP/GOx cascade system, fluorescence intensity at 410 nm is observed with 23 fold increments whereas the increase in fluorescence intensity for HRP/uricase system is about 20 fold at 410 nm. Gradual increase in fluorescence intensity at the initial condition and reached to equilibrium at higher concentration of bioanalytes is observed for the cascade systems (Figure 2, Figure S6). Bio-analytes (glucose or uric acid) act as a source of H<sub>2</sub>O<sub>2</sub> in presence of their corresponding oxidases, which initiate the cross-coupling of tyrosine [51] of BTCA-Y in presence of HRP.

H<sub>2</sub>O<sub>2</sub> produced by oxidase/HRP cascade reaction [52] in presence of biological species (i.e., glucose or uric acid) was detected precisely using fluorogenic technique (Figure 3 and Figure S6). The response of bioanalytes was verified by performing several control experiments (Figure 3b). Initially, BTCA-Y solution was prepared without HRP in presence of GOx/glucose. However, the composite didn't respond in fluorescence. Later HRP mediated BTCA-Y was tested with GOx/glucose and positive response was obtained. Other two HRP mediated systems containing only glucose or only GOx didn't respond (Figure 3b). HRP/BTCA-Y hybrid solution in presence of both GOx and glucose responded significantly using fluorogenic techniques and showed optical response under UV light. The H<sub>2</sub>O<sub>2</sub> produced by GOx/glucose hybrid oxidizes the phenolic -OH present in BTCA-Y to form cross-

linked fluorescent polymeric aggregates. Similarly, fluorescence response was also obtained using uricase/uric acid hybrid system. The BTCA-Y responds to HRP when the analytes coupled with their corresponding oxidase enzymes e.g. uric acid produces  $H_2O_2$  in presence of uricase and glucose produces  $H_2O_2$  in presence of GOx (Figure 3b and Figure S7).

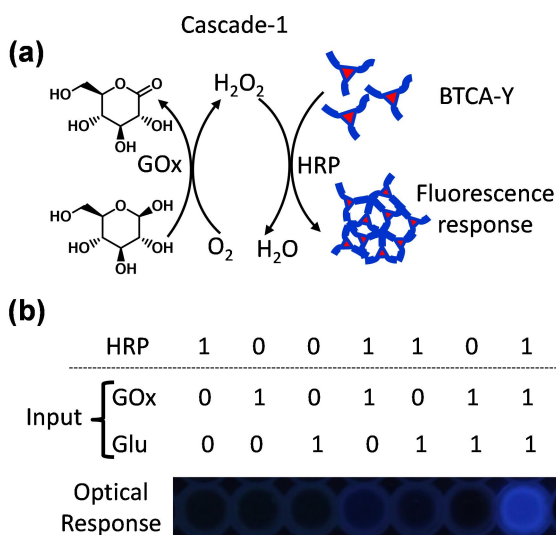


**Figure 3.** (a) Overall enzymatic cascade reaction pathways using HRP/GOx in presence of glucose (Glu) and formation of fluorescent dityrosine crosslinked polymer are shown. (b) Combination of enzyme (HRP) and Input (GOx and Glu) used for cascade reaction. Boolean number “1”, “0” represent presence and absence of HRP, input (GOx and Glu) and output as optical response respectively under UV light (365 nm).

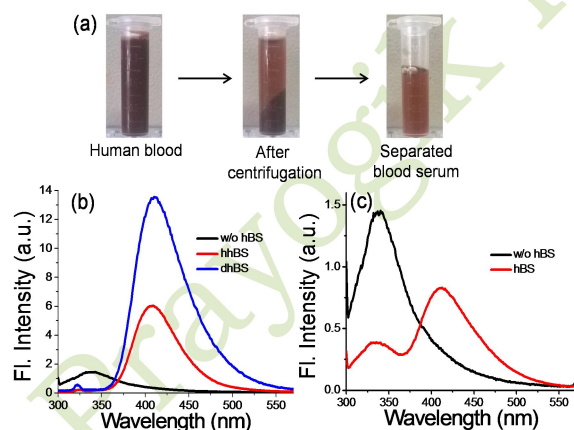


**Figure 4.** (a) Showing collection of healthy human blood. Blood serum gets separated after centrifugation and serum was collected for the study. (b) shows increased fluorescence intensity at 410 nm with healthy human blood serum (hhBS), diabetic human blood serum (dhBS) with increase in glucose concentration and (c) represents fluorescence spectra of healthy human blood serum (hBS) which detects the uric acid containing blood serum. Reaction time was fixed as 7 min for all the experiments.

## Glucose and uric acid detection from blood serum

For potential application in clinical diagnosis, healthy human blood was collected. Previously, diluted blood serum was analyzed to detect the glucose level using ultra-small Pt nanocluster [53]. In this work, we have directly used the isolated blood serum. The healthy human blood serum (hhBS) was isolated using centrifugation technique (Figure 4). Healthy human (male) blood contains 5-6  $\mu\text{mol mL}^{-1}$  of glucose in fasting condition and on diabetic condition the level increases to 9-10  $\mu\text{mol mL}^{-1}$  [54]. Whereas, uric acid level for healthy human (male) is about 0.16  $\mu\text{mol mL}^{-1}$  to 0.5  $\mu\text{mol mL}^{-1}$  [55]. We first tested with pure blood serum and significant response from the developed system was found for both the cases. The observed results are comparable with the amount  $4\pm 0.15 \mu\text{mol mL}^{-1}$  of glucose and  $0.5\pm 0.3 \mu\text{mol mL}^{-1}$  of uric acid. Further, we have tested with the elevated analyte level in blood serum. The elevated amount of glucose (10  $\mu\text{mol mL}^{-1}$ ) in blood serum was also detected at different concentrations. Further, we were motivated to utilize the developed system in direct detection of diabetic blood sugar level. We have collected the diabetic human blood serum (dhBS) and checked the sugar level by colorimetric method (Figure S9). The sugar concentration was calculated as 206 mg/dL ( $\sim 11.6 \mu\text{mol mL}^{-1}$ ). Here, our developed method was employed for the detection of sugar concentration, which is calculated as  $201\pm 0.2 \text{ mg/dL}$  ( $\sim 11.2 \mu\text{mol mL}^{-1}$ ) from comparative fluorescence intensity. Both the obtained data from colorimetric method (Figure S8) and our developed method is close to each other. Therefore, the hybrid BTCA-Y/HRP could be used to detect the glucose and uric acid level precisely which can be assessed using fluorescence and optical response method under UV light ( $\lambda = 365 \text{ nm}$ ) with blue light emission.

## 4. Conclusions

In summary, we have developed an effective bio-molecule based fluorogenic probe for the detection of  $H_2O_2$  generated by bio-analytes (i.e. glucose and uric acid), which are present in blood serum. The cascade reactions based on polymeric nanospheres (diameter of 100 nm) detect various bio-analytes in single platform with a very short time frame (7 minutes) by the detection of in-situ produced  $H_2O_2$ . The developed method is very suitable for the diagnosis of glucose ( $4\pm 0.15 \mu\text{mol mL}^{-1}$ ) and uric acid ( $0.5\pm 0.3 \mu\text{mol mL}^{-1}$ ) from healthy human blood serum. So the higher amount of glucose ( $5 \mu\text{mol mL}^{-1}$ ,  $11.2 \mu\text{mol mL}^{-1}$ ) was detected very easily. Therefore, the developed system is found very efficient for the diagnosis of higher amount of glucose and uric acid level. We have used our system to analyze the diabetic blood serum. We have calculated the sugar level as  $\sim 201 \text{ mg/dL}$  which is very similar to the colorimetrically estimated glucose value (206 mg/dL). Therefore, this method is very efficient for the diagnosis the issues caused by the diseases associated with gout and diabetic conditions. We believe that this approach will hold a place in biochemical study as fluorogenic polymeric probe in near future.

## 5. Acknowledgements

Authors acknowledge the sophisticated instrumentation Centre (SIC), IIT Indore for providing access to the instrumentation. S. Bhowmik is indebted to DST Inspire and S. Biswas is indebted to UGC for their fellowship. Authors thank to Dr. Hamendra S. Parmar and Dr. Narendra Kumar, DAVV, Indore for their help during biological experiments. SAIF, IIT Bombay is also acknowledged for the assistance of EM facility.

## 6. Notes and References

- N. Li, A. Than, X. Wang, S. Xu, L. Sun, H. Duan, C. Xu, P. Chen, Ultrasensitive Profiling of Metabolites Using Tyramine-Functionalized Graphene Quantum Dots. *ACS Nano* 10 (2016) 3622-3629.
- S. Ye, J. J. Hu, Q. A. Zhao, D. Yang, Fluorescent probes for in vitro and in vivo quantification of hydrogen peroxide, *Chem. Sci.*, 11, (2020) 11989-11997.
- M. S. Messina, G. Quargnali, C. J. Chang. Activity-Based Sensing for Chemistry-Enabled Biology: Illuminating Principles, Probes, and Prospects for Boronate Reagents for Studying Hydrogen Peroxide. *ACS Bio & Med Chem Au*, 2, (2022) 548-564.
- C. B. Dickinson, C. J. Chang, Chemistry and Biology of Reactive Oxygen Species in Signaling or Stress Responses. *Nat. Chem. Biol.* 7 (2011) 504-511.
- R. S. Arnold, J. Shi, E. Murad, A. M. Whalen, C. Q. Sun, R. Polavarapu, S. Parthasarathy, J. A. Petros, J. D. Lambeth, Hydrogen Peroxide Mediates the Cell Growth and Transformation Caused by the Mitogenic Oxidase Nox1. *Proc. Natl. Acad. Sci. U. S. A.* 98 (2001) 5550-5555.
- H. Peng, T. Wang, G. Li, J. Huang, Q. Yuan. Dual-Locked Near-Infrared Fluorescent Probes for Precise Detection of Melanoma via Hydrogen Peroxide-Tyrosinase Cascade Activation. *Anal. Chem.* 94 (2022) 1070-1075.
- K.J. Harrington, P. Nenclares, The biology of cancer, *Medicine*, 51 (2023) 1-6.
- V. Veschi, A. Turdo, C. Modica, F. Verona, S. D. Franco, M. Gaggianesi, E. Tirrò, S. D. Bella, M. L. Iacono, V. D. Pantina, G. Porcelli, L. R. Mangiapane, P. Bianca, A. Rizzo, E. Sciacca, I. Pillitteri, V. Vella, A. Belfiore, M. R. Bongiorno, G. Pistone, L. Memeo, L. Colarossi, D. Giuffrida, C. Colarossi, P. Vigneri, M. Todaro, G. Stassi, Recapitulating thyroid cancer histotypes through engineering embryonic stem cells. *Nat Commun.* 14 (2023) 1351.
- A. A. Alfadda, R. M. J. Sallam, Reactive Oxygen Species in Health and Disease. *J. Biomed. Biotechnol.* 2012 (2012) 936486.
- Y. Dong, Q. Hou, J. Lei, P. G. Wolf, H. Ayansola, B. Zhang, Quercetin Alleviates Intestinal Oxidative Damage Induced by H<sub>2</sub>O<sub>2</sub> via Modulation of GSH: In Vitro Screening and In Vivo Evaluation in a Colitis Model of Mice. *ACS Omega* 5 (2020) 8334-8346.
- Z. Mao, Z. Qing, T. Qing, F. Xu, L. Wen, X. He, D. He, H. Shi, K. Wang, Poly(thymine)-Templated Copper Nanoparticles as a Fluorescent Indicator for Hydrogen Peroxide and Oxidase-based Biosensing. *Anal. Chem.* 87 (2015) 7454-7460.
- H. Zeng, W. Qiu, L. Zhang, R. Liang, J. Qiu, Lanthanide Coordination Polymer Nanoparticles as an Excellent Artificial Peroxidase for Hydrogen Peroxide Detection. *Anal. Chem.* 88 (2016) 6342-48.
- L. Tang, S. Mo, S. G. Liu, N. Li, Y. Ling, N. B. Li, H. Q. Luo, Preparation of bright fluorescent polydopamine-glutathione nanoparticles and their application for sensing of hydrogen peroxide and glucose. *Sensors and Actuators B* 259 (2018) 467-474.
- B. Li, J.-B. Chen, Y. Xiong, X. Yang, C. Zhao, J. Sun, Development of turn-on fluorescent probes for the detection of H<sub>2</sub>O<sub>2</sub> vapor with high selectivity and sensitivity. *Sensors and Actuators B* 268 (2018) 475-484.
- X. Liu, H. Tian, L. Yang, Y. Su, M. Guo, X. Song. A sensitive and selective fluorescent probe for the detection of hydrogen peroxide with a red emission and a large Stokes shift. *Sensors and Actuators B* 255 (2018) 1160-1165.
- Y. Shen, X. Zhang, Y. Zhang, Y. Wu, C. Zhang, Y. Chen, J. Jin, H. Li, A mitochondria-targeted colorimetric and ratiometric fluorescent probe for hydrogen peroxide with a large emission shift and bio-imaging in living cells. *Sensors and Actuators B* 255 (2018) 42-48.
- P. Wang, K. Wang, Y. Gu, A highly selective fluorescent turn-on NIR probe for the bioimaging of hydrogen peroxide in vitro and in vivo. *Sensors and Actuators B* 228 (2016) 174-179.
- M. S. Purdey, H. J. McLennan, M. L. Sutton-McDowall, D. W. Drumm, X. Zhang, P. K. Capon, S. Heng, J. G. Thompson, A. D. Abell, Biological hydrogen peroxide detection with aryl boronate and benzil BODIPY-based fluorescent probes. *Sensors and Actuators B* 262 (2018) 750-757.
- S. I. Reja, M. Gupta, N. Gupta, V. Bhalla, P. Ohri, G. Kaur, M. Kumar, A lysosome targetable fluorescent probe for endogenous imaging of hydrogen peroxide in living cells. *Chem. Commun.* 53 (2017) 3701-3704.
- E. K. Lim, T. Kim, S. Paik, S. Haam, Y. M. Huh, K. Lee, Nanomaterials for Theranostics: Recent Advances and Future Challenges. *Chem. Rev.* 115 (2015) 327-394.
- Z. Song, R. T. K. Kwok, D. Ding, H. Nie, J. W. Y. Lam, B. Liuc, B. Z. Tang, An AIE-active fluorescence turn-on bioprobe mediated by hydrogen-bonding interaction for highly sensitive detection of hydrogen peroxide and glucose. *Chem. Commun.* 52 (2016) 10076-10079.
- L. Ding, S. Chen, W. Zhang, Y. Zhang, X.-d. Wang, Fully Reversible Optical Sensor for Hydrogen Peroxide with Fast Response. *Anal. Chem.* 90 (2018) 7544-7551.
- X. Li, J. Li, Y. Tao, Z. Peng, P. Lu, Y. Wang, Oxazole-based high resolution ratiometric fluorescent probes for hydrogen peroxide detection. *Sensors and Actuators B* 247 (2017) 609-616.
- S. Choi, S. Park, K. Lee, J. Yu, Oxidant-resistant imaging and ratiometric luminescence detection by selective oxidation of silver nanodots. *Chem. Commun.* 49 (2013) 10908-10910.
- S. K. Bhunia, S. Dolai, H. Sun, R. Jelinek, "On/off/on" hydrogen-peroxide sensor with hemoglobin-functionalized carbon dots. *Sensors and Actuators B* 270 (2018) 223-230.
- P. Marks, B. Radaram, M. Levine, I. A. Levitsky, Highly Efficient Detection of Hydrogen Peroxide in Solution and in the Vapor Phase via Fluorescence Quenching. *Chem. Commun.* 51 (2015) 7061-7064.
- A. T. Franksa, K. J. Franz, A prochelator with a modular masking group featuring hydrogen peroxide activation with concurrent fluorescent reporting. *Chem. Commun.* 50 (2014) 11317-11320.

28. N. Karton-Lifshin, E. Segal, L. Omer, M. Portnoy, R. S. Fainaro, D. Shabat, A Unique Paradigm for a Turn-ON Near-Infrared Cyanine-Based Probe: Noninvasive Intravital Optical Imaging of Hydrogen Peroxide. *J. Am. Chem. Soc.* 133 (2011) 10960-10965.
29. D. Wu, A. C. Sedgwick, T. Gunnlaugsson, E. U. Akkaya, J. Yoon, T. D. James, Fluorescent Chemosensors: The Past, Present and Future. *Chem. Soc. Rev.* 46 (2017) 7105-7123.
30. C. Feng, F. Wang, Y. Dang, Z. Xu, H. Yu, W. Zhang, A Self-Assembled Ratiometric Polymeric Nanoprobe for Highly Selective Fluorescence Detection of Hydrogen Peroxide. *Langmuir* 33 (2017) 3287-3295.
31. Y. Zhang, X. Yanga, Z. Gao, In Situ Polymerization of Aniline on Carbon Quantum Dots: A New Platform for Ultrasensitive Detection of Glucose and Hydrogen Peroxide. *RSC Adv.* 5 (2015) 21675-21680.
32. G. C. Van de Bittner, E. A. Dubikovskaya, C. R. Bertozzi, C. J. Chang, In Vivo Imaging of Hydrogen Peroxide Production in a Murine Tumor Model with a Chemoselective Bioluminescent Reporter. *Proc. Natl. Acad. Sci. U. S. A.* 107 (2010) 21316-21321.
33. W-K. Oh, Y. S. Jeong, S. Kim, J. Jang, Fluorescent Polymer Nanoparticle for Selective Sensing of Intracellular Hydrogen Peroxide. *ACS Nano* 6 (2012) 8516-8524.
34. B. D. Ulery, L. S. Nair, C. T. Laurencin, Biomedical Applications of Biodegradable Polymers. *J. Polym. Sci. B. Polym. Phys.* 49 (2011) 832-864.
35. X. Wang, J. Hu, G. Zhang, S. Liu, Highly Selective Fluorogenic Multianalyte Biosensors Constructed via Enzyme-Catalyzed Coupling and Aggregation-Induced Emission. *J. Am. Chem. Soc.* 136 (2014) 9890-9893.
36. S.-I. Shoda, H. Uyama, J.-I. Kadokawa, S. Kimura, S. Kobayashi, Enzymes as Green Catalysts for Precision Macromolecular Synthesis. *Chem. Rev.* 116 (2016) 2307-2413.
37. S. Biswas, R. G. Jadhav, A. K. Das, Construction of Porous Organic Nanostructures using Cooperative Self-assembly for Lipase Catalyzed Inclusion of Gastrodigenin. *ACS Appl. Nano Mater.* 1 (2018) 175-182.
38. A. Lampel, S. A. McPhee, H.-A. Park, G. G. Scott, S. Humagain, D. R. Hekstra, B. Yoo, P. W. J. M. Frederix, T.-D. Li, R. R. Abzalimov, S. G. Greenbaum, T. Tuttle, C. Hu, C. J. Bettinger, R. V. Uljin, Polymeric Peptide Pigments with Sequence-Encoded Properties. *Science* 356 (2017) 1064-1068.
39. T. Kamperman, S. Henke, B. Zoetebier, N. Ruitenkamp, R. Wang, B. Pouran, H. Weinans, M. Karperien, J. Leijten, Nanoemulsion-Induced Enzymatic Crosslinking of Tyramine-Functionalized Polymer Droplets. *J. Mater. Chem. B* 5 (2017) 4835-4844.
40. Y. Lee, J. W. Bae, J. W. Lee, W. Suh, K. D. Park, Enzyme-Catalyzed In Situ Forming Gelatin Hydrogels as Bioactive Wound Dressings: Effects of Fibroblast Delivery on Wound Healing Efficacy. *J. Mater. Chem. B* 2 (2014) 7712-7718.
41. N. Q. Tran, Y. K. Joung, E. Lih, K. D. Park, In Situ Forming and Rutin-Releasing Chitosan Hydrogels as Injectable Dressings for Dermal Wound Healing. *Biomacromolecules* 12 (2011) 2872-2880.
42. G. S. Harms, S. W. Pauls, J. F. Hedstrom, C. K. Johnson, Fluorescence and Rotational Dynamics of Dityrosine. *J. Fluoresc.* 7 (1997) 283-292.
43. N. Li, A. Than, X. Wang, S. Xu, L. Sun, H. Duan, C. Xu, P. Chen, Ultrasensitive Profiling of Metabolites Using Tyramine-Functionalized Graphene Quantum Dots. *ACS Nano* 10 (2016) 3622-3629.
44. T. Michon, M. Chenu, N. Kellershon, M. Desmadril, J. Gueguen, Horseradish Peroxidase Oxidation of Tyrosine-Containing Peptides and Their Subsequent Polymerization: A Kinetic Study. *Biochemistry* 36 (1997) 8504-8513.
45. W. Zhang, W. Liu, P. Li, F. Huang, H. Wang, B. Tang, Rapid-Response Fluorescent Probe for Hydrogen Peroxide in Living Cells Based on Increased Polarity of C-B Bonds. *Anal. Chem.* 87 (2015) 9825-9828.
46. J. Qiao, Z. Liu, Y. Tian, M. Wu, Z. Niu, Multifunctional Self-Assembled Polymeric Nanoprobes for FRET-Based Ratiometric Detection of Mitochondrial H<sub>2</sub>O<sub>2</sub> in Living Cells. *Chem. Commun.* 51 (2015) 3641-3644.
47. E. S. Lee, V. G. Deepagan, D. G. You, J. Jeon, G-R. Yi, J. Y. Lee, D. S. Lee, Y. D. Suh, J. H. Park, Nanoparticles Based on Quantum Dots and a Luminol Derivative: Implications for In Vivo Imaging of Hydrogen Peroxide by Chemiluminescence Resonance Energy Transfer. *Chem. Commun.* 52 (2016) 4132-4135.
48. F. He, Y. Tang, M. Yu, S. Wang, Y. Li, D. Zhu, Fluorescence-Amplifying Detection of Hydrogen Peroxide with Cationic Conjugated Polymers, and Its Application to Glucose Sensing. *Adv. Funct. Mater.* 16 (2006) 91-94.
49. O. Ikkala, G. ten Brinke, Functional Materials Based on Self-Assembly of Polymeric Supramolecules. *Science* 295 (2002) 2407-2409.
50. S. J. Rowan, Polymer Self-assembly: Micelles Make a Living. *Nat. Mater.* 8 (2009) 89-91.
51. K. Minamihata, M. Goto, N. Kamiya, Site-Specific Protein Cross-Linking by Peroxidase-Catalyzed Activation of a Tyrosine-Containing Peptide Tag. *Bioconjug. Chem.* 22 (2011) 74-81.
52. Y. Zhang, S. Tsitkov, H. Hess, Proximity Does not Contribute to Activity Enhancement in the Glucose Oxidase-Horseradish Peroxidase Cascade. *Nat. Commun.* 7 (2016) 13982.
53. L. Jin, Z. Meng, Y. Zhang, S. Cai, Z. Zhang, C. Li, L. Shang, Y. Shen, Ultrasmall Pt Nanoclusters as Robust Peroxidase Mimics for Colorimetric Detection of Glucose in Human Serum. *ACS Appl. Mater. Inter.* 9 (2017) 10027-10033.
54. D. Giugliano, A. Ceriello, K. Esposito, Glucose Metabolism and Hyperglycemia. *Am. J. Clin. Nutr.* 87 (2008) 217S-225S.
55. V. A. Buzanovskii, Determination of Uric Acid in Blood. *Rev. J. Chem.* 5 (2015) 281-323.

## 7. About the author(s)

Apurba K. Das is currently working as a Professor at Indian Institute of Technology Indore. He completed his PhD from Indian Association for the Cultivation of Science, Kolkata in 2006. After his postdoctoral research associate positions at the University of Manchester, UK and Strathclyde University, Glasgow, UK, he joined Indian Institute of Technology Indore



in 2009. His current research interests are broadly in the areas of supramolecular organic materials for applications in biology and electrocatalysis. He is a Fellow of the Royal Society of Chemistry (FRSC), UK.

**Article Note:** A collection of invited papers based on *Award Lecture* presentations in the International webinar *Science Beyond Boundary: Invention, Discovery, Innovation and Society 'Rasayan 15'* held online on December 10, 2022.